Late stages of spinodal decomposition in a three-dimensional model system

Amitabha Chakrabarti* and Raúl Toral†
Department of Physics and Center for Advanced Computational Science, Temple University, Philadelphia, Pennsylvania 19122

James D. Gunton
Department of Physics, Lehigh University, Bethlehem, Pennsylvania 18015
(Received 19 September 1988)

We present results from a numerical study of the Cahn-Hilliard model for spinodal decomposition in a three-dimensional system. Details of the numerical integration method and the late-time field configurations are discussed. We find that the late-time behavior of the system is well described in terms of scaling with a characteristic length, $R(t)$. The data for both the pair-correlation function and the structure function show scaling behavior at sufficiently late times. The time dependence of $R(t)$ is analyzed extensively and found to be consistent with a modified Lifshitz-Slyozov law; i.e., $R(t)=c+dt^{1/3}$.

I. INTRODUCTION

The phenomenon of spinodal decomposition corresponding to a small-amplitude, long-wavelength instability appears in many binary mixtures following a quench deep inside the coexistence curve. At later times, the small inhomogeneities in the order parameter evolve into macroscopic domains of one or the other phase, and an interconnected structure is formed. The theoretical understanding of this process of phase separation,[1] is based mainly on the Cahn-Hilliard-Cook (CHC)[2] formulation. Analytical studies of this field-theoretic model have been reasonably successful in describing the early-time regime of the phase-separation process[3–5] but, due to their approximate nature, they are not as useful in the so-called late stages. This late-time regime is characterized by the coarsening of domains separated by interfaces whose thickness is proportional to the equilibrium correlation length. Also, the well-known Lifshitz-Slyozov[6] theory and its later extensions,[7–8] which all assume a small volume fraction of one of the two phases, are not strictly applicable to the case of a critical quench. It seems then that numerical simulation would play a useful role, at least for the present time, in our ability to understand and to predict the late-time behavior of such a complicated system. Numerical simulations traditionally have focussed mainly on discrete models[9,10] (Ising type) with a microscopic dynamics of spin exchange (Kawasaki dynamics) which conserves the order parameter. The CHC model can be "derived" from this kinetic Ising model, but the derivation involves several approximations which, while plausible, have not yet been rigorously justified. Indeed, recent studies[11–13] have predicted that the CHC and Ising models belong to different universality classes. Numerical studies, however, of both the Ising model[10,14] and the CHC model in two dimensions[15,16] (and an alternative cell-dynamics version[17,18] of the CHC model) have suggested that the time-dependent behavior of the characteristic size of the domains (as characterized by a power-law behavior in time) and the scaling function derived from the pair-correlation function are the same within the numerical accuracy of the studies.[19] In three dimensions the only numerical results available so far are those from earlier pioneering Monte Carlo simulations of Kawasaki dynamics in the Ising model.[9] In this paper we report results obtained from a numerical integration of the CHC model. It turns out that the numerical simulation of this model is very demanding in terms of computer resources (both central-processing-unit time and central memory) which makes a totally definitive solution of this problem inaccessible. However, useful new results have been obtained using a Cray X-MP48 and have been reported by us in a recent short paper.[20] Here we present the details of this work including more extensive analysis of the data than presented in the short paper. The outline of the paper is as follows: In Sec. II we introduce the model and the numerical methods used in the integration of the equations. In Sec. III we present the results for the morphology and the profile of the interfaces of the system, the scaling with time of the pair-correlation function, the structure factor, and the time dependence of a characteristic length. Section IV presents the main conclusions of our study.

II. MODEL AND NUMERICAL METHODS

The theory developed by Cahn, Hilliard, and Cook[2] for the spinodal decomposition mechanism for phase-separation processes relates the time variation of the conserved concentration field $\phi(\mathbf{x},\tau)$ to the functional derivative of a (coarse-grained) free-energy functional plus a thermal noise in the following way:

$$\frac{\partial\phi(\mathbf{x},\tau)}{\partial\tau}=M\nabla^2\frac{\delta F}{\delta\phi}+\eta(\mathbf{x},\tau)\ . \tag{1}$$

The functional $F[\phi]$ for binary alloy systems is usually assumed to have the Ginsburg-Landau form:

$$F=\tfrac{1}{2}\int d\mathbf{x}\left[K|\nabla\phi|^2-b\phi^2+\frac{u}{2}\phi^4\right], \tag{2}$$

where M is the mobility (assumed to be a constant) and r, u, and K are phenomenological positive parameters. The thermal noise $\eta(\mathbf{x},\tau)$ is a Gaussian random variable satisfying the fluctuating dissipation theorem

$$\langle \eta(\mathbf{x},\tau)\eta(\mathbf{x}',\tau')\rangle = -2k_B TM\nabla^2\delta(\mathbf{x}-\mathbf{x}')\delta(\tau-\tau') , \quad (3)$$

where $\langle \cdots \rangle$ denotes an ensemble average. Equations (1)–(3) define what is known as model B in the terminology of critical phenomena.[21] The resulting equation of motion obtained after substituting Eq. (2) into Eq. (1) is

$$\frac{\partial\phi}{\partial\tau} = M\nabla^2(-b\phi+u\phi^3-K\nabla^2\phi)+\eta . \quad (4)$$

Following Grant *et al.*,[5] this equation can be written in a much simpler fashion by suitable rescaling of the field by its mean-field correlation value, the distances by the mean-field correlation length and time by the time taken to diffuse one correlation length, i.e.,

$$\mathbf{r} = \frac{\mathbf{x}}{\sqrt{K/b}} , \quad (5a)$$

$$t = \frac{\tau}{K/2Mb^2} , \quad (5b)$$

$$\psi = \frac{\phi}{\sqrt{b/u}} . \quad (5c)$$

The resulting dimensionless equation is

$$\frac{\partial\psi}{\partial t} = \tfrac{1}{2}\nabla^2(-\nabla^2\psi-\psi+\psi^3)+\sqrt{\epsilon}\nu , \quad (6)$$

with $\epsilon=(k_B Tu/b^2)(b/K)^{d/2}$, and the new Gaussian noise $\nu(\mathbf{r},t)$ satisfies

$$\langle \nu(\mathbf{r},t)\nu(\mathbf{r}',t')\rangle = -\nabla^2\delta(\mathbf{r}-\mathbf{r}')\delta(t-t') . \quad (7)$$

At low temperatures, the role of the noise term is thought to be very small and does not affect the late stages of the evolution, as pointed out in the studies of the two-dimensional version of the model.[15,16] In this regime (low temperature and late stages) the effect of the noise is simply a roughening of the interfaces which is believed not to affect either the growth law of the typical domain size or the form of the scaling function. Equation (4), without the presence of the noise term, is known as the Cahn-Hilliard equation[2] and it is the object of study of this paper.

Numerically solving Eq. (6) in three dimensions is a very demanding task, even in the absence of the noise term. Here a finite difference scheme for both the spatial and temporal derivatives has been used. The spatial discretization is achieved by replacing the continuous space of position vectors $\mathbf{r}=(x,y,z)$ by a simple cubic lattice with $N=L^3$ sites and lattice spacing δr (periodic boundary conditions are assumed in order to avoid surface effects). The Laplacian operator is then approximated by the expression

$$\nabla^2 f(x,y,z) = \delta r^{-2}[f(x+\delta r,y,z)+f(x-\delta r,y,z)+f(x,y+\delta r,z) + f(x,y-\delta r,z)+f(x,y,z+\delta r)+f(x,y,z-\delta r)-6f(x,y,z)] , \quad (8)$$

which is accurate to order δr^2. We integrate numerically Eq. (6) without the noise term by using a first order Euler scheme:

$$\psi(\mathbf{r},t+dt) = \psi(\mathbf{r},t)+dt\frac{\partial\psi}{\partial t} . \quad (9)$$

In order to carry out the calculations within a reasonable amount of computer time one would like to choose a large time step and a moderately large system size. However, the discretized version of Eq. (6) (considered as a coupled map) develops a subharmonic bifurcation kind of instability for large time steps. A linear stability analysis[16] shows that this bifurcation can be avoided by choosing the parameters dt and δr such that the following inequality is satisfied (in three dimensions):

$$dt < \frac{\delta r^4}{36-3\delta r^2} . \quad (10)$$

This simple criterion turns out to be a necessary but not sufficient condition for the stability of the numerical integration. We have chosen in our simulation $\delta r = 1.7$ and $dt = 0.1$. This value of dt is more than three times small than the "safe" value of dt predicted by Eq. (10). We have studied the effect of reducing the value of the time step dt with the conclusion that, even though particular numerical values of the field variable (mainly along the interfaces) might depend on the choice of dt, smaller values of dt do not change quantities that express a global behavior, such as the structure function, the pair correlation function, or the typical domain size. Using $dt = 0.01$ for example, produces a change in the domain size less than 0.1%, which is well within our statistical errors.

We have considered a simple cubic lattic with $N=L^3$ points with $L=66$, which is equivalent to saying that the linear dimension of the system (in the dimensionless units described before) is $66\delta r \approx 112$. We choose the initial field configurations to be uniformly distributed between -0.125 and 0.125, with order parameter equal to zero (i.e., a critical quench). In order to average over to initial random configurations we have performed 46 runs out to $t=10\,000$ and 25 runs out to $t=20\,000$. By comparing the domain sizes at the latest time we conclude that we are at a considerably later stage of evolution than previous Monte Carlo results,[9] although the comparison is subtle as discussed later. As well, our system size is larger than that used in the Monte Carlo studies.

III. RESULTS

A. Late-time field configurations

The characteristic interconnected structure of a system at a late stage of spinodal decomposition is clearly visible

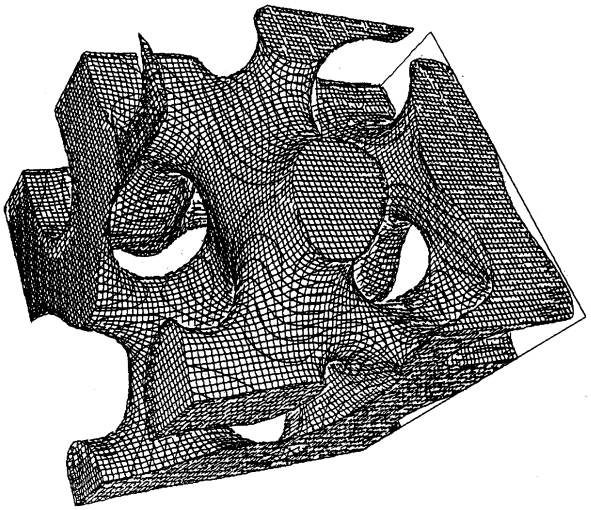

FIG. 1. Snapshot of the system configuration at $t=20\,000$. The region with a positive value for the concentration field is indicated opaque, while the region with a negative value is transparent. The spanning structure characteristic of spinodal decomposition is clearly visible.

in Fig. 1. In this figure positive (negative) values of the field ψ are presented by opaque (transparent) points. We note that both phases form complementary spanning structures, which is similar to that observed in experiments on binary systems.[22]

The probability distribution for the field $\psi(\mathbf{r},t)$ is plotted in Fig. 2 for two late times during the evolution. We note that the distribution is very sharply peaked around the equilibrium values of ψ, i.e, -1 and $+1$. This indicates that the field is in local equilibrium spatially except at the interfaces. The probability distribution function $P(\psi(\mathbf{r},t))$ contains information about the interfaces.[23] A simple heuristic argument allows us to relate $P(\psi(\mathbf{r},t))$ to the interface profile: Across the interface one can approximately replace $P(\psi)d\psi$ simply by $R(t)^{-1}dr$, where $R(t)$ is a typical measure of the domain size, so that

$$F(\psi)\equiv\int_{-1}^{\psi(r)}P(\psi)d\psi-\tfrac{1}{2}=\frac{1}{R(t)}\int_{-[R(t)/2]}^{r}dr-\tfrac{1}{2}\ . \quad (11)$$

Thus, one finds

$$\psi(r)=f^{-1}(r/R(t))\ .$$

In Fig. 3 we plot the interface profile for two late times derived by the method explained earlier, using for $R(t)$ the first zero of the pair correlation function (see Sec. III C) together with the asymptotic profile $\psi(r)=\tanh(r/\sqrt{2})$. It seems that the interface profile is essentially independent of time and well approximated by the hyperbolic tangent fit. We also note that the width of the interface is of the order of 1.0 and thus is about 4% of the maximum domain size. Since this number is small, we believe that the system studied here is in an advanced stage of the evolution process.

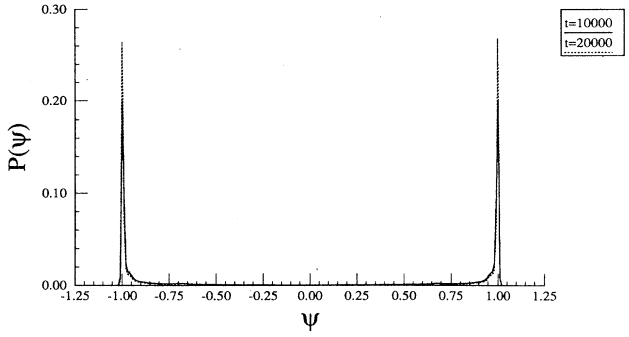

FIG. 2. Probability distribution $P(\psi(\mathbf{r},t))$ at two advanced times during the system evolution. Note that the distribution for both times is sharply peaked around the equilibrium values for the field, $+1$ and -1.

B. Scaling

The late stages of the dynamical process can be described in terms of an asymptotic scaling with a time-dependent length.[1,9,24,25] The fundamental assumption is that in the asymptotic scaling regime only one length, $R(t)$, is relevant. This length, $R(t)$, represents the characteristic size of the one-phase domains. Dynamical scaling has been traditionally analyzed in terms of the structure function, $S(\mathbf{k},t)$:

$$S(\mathbf{k},t)=\left\langle\frac{1}{N}\sum_{\mathbf{r}}\sum_{\mathbf{r}'}e^{ik\cdot r}[\psi(\mathbf{r}+\mathbf{r}')\psi(\mathbf{r}')-\langle\psi\rangle^2]\right\rangle\ , \quad (12)$$

where the sums run over the lattice and $\mathbf{k}=(2\pi/L\delta r)\boldsymbol{\mu}$ belong to the first Brillouin zone in the reciprocal space,

$$\boldsymbol{\mu}=(\mu_x,\mu_y,\mu_z);\mu_x,\mu_y,\mu_z=0,1,\ldots,L-1\ .$$

More recently, though, scaling has also been studied with the pair-correlation function, $G(\mathbf{r},t)$:

$$G(\mathbf{r},t)=\sum_{\mathbf{k}}e^{i\mathbf{k}\cdot\mathbf{r}}S(\mathbf{k},t)\ , \quad (13)$$

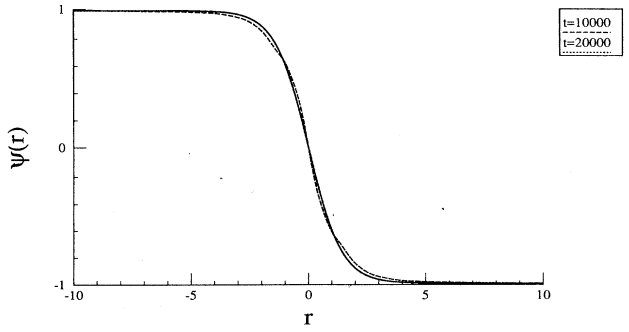

FIG. 3. Interface profile derived from an integration of the probability distribution $P(\psi(\mathbf{r},t))$ in Fig. 1 according to Eq. (11). The curves for $t=10\,000$ and $t=20\,000$ actually fall on top of each other indicating that the interfaces have probably the equilibrium shape by $t=10\,000$. The solid line is the planar interface equilibrium soliton solution $\psi(r)=\tanh(r/\sqrt{2})$.

even though this function has the disadvantage that it is not experimentally observable. The dynamical scaling hypothesis states that

$$G(\mathbf{r},t)=g(\mathbf{r}/R(t)) \tag{14}$$

and

$$S(\mathbf{k},t)=R(t)^d F(\mathbf{k}R(t)) , \tag{15}$$

where both $g(\rho)$ and $F(\chi)$ are time-dependent functions.

1. Pair correlation function

We have performed a spherical average of the pair-correlation function

$$G(r,t)=\sum_{-r(\Delta r/2)<|\mathbf{r}|\le r+(\Delta r/2)} G(\mathbf{x},t) \Big/ \sum_{r-(\Delta r/2)<|\mathbf{r}|\le r+(\Delta r/2)} 1 . \tag{16}$$

For a given large r, the sums in this equation contain a large number of points (of the order of $4\pi r^2\Delta r$) and (if Δr is not too small) the corresponding $G(r,t)$ is a smooth and well behaved function of r and t with small statistical errors. However, this procedure has the disadvantage that a simple point r represents an average over a spherical shell of width Δr, introducing an uncertainty in the coordinate R of the order of $\Delta r/2$. We also studied the correlation function averaged along the lattice axes, i.e.,

$$G_a(x,t)=\tfrac{1}{3}[G(\mathbf{r}=(x,0,0),t)+G(\mathbf{r}=(0,x,0),t)+G(\mathbf{r}=(0,0,x),t)] . \tag{17}$$

The domain morphology for the conserved order parameter produces a damped oscillatory behavior in both $G(r,t)$ and $G_a(x,t)$. This allows one to give a quantitative measure of the domain size as the location of the first zero of the correlation function.[26] The length $R_g(t)$ ($R_a(t)$) was calculated fitting the four points in $G(r,t)$($G_a(x,t)$) closest to its first zero (of which two fall on each side of its first zero) to a cubic polynomial of r (x) and defining $R_g(t)$ ($R_a(t)$) as the value of r (x) where this fitted function vanishes.

Fig. 4 shows the scaling behavior of $G(r,t)$ with $R_g(t)$ as the scaling length. The scaling hypothesis seems to be extremely well satisfied, over the whole range of values of r, particularly at late time. On the other hand, a detailed analysis of the first minimum of $G(r,t)$ shows that the position of this minimum does not change with time but that the value of the minimum decreases systematically, at least up to $t=15\,000$, see Fig. 5. Also, the value of the scaling function $g(z)$ in Fig. 4 at the origin is increasing slowly with time. For $z=0$ the value of this function is equal to the equilibrium value of the pair-correlation function at $r=0$, which is given by the second moment of the field distribution

$$g(0)=G(0,\infty)=\overline{\psi^2(t=\infty)} , \tag{18}$$

where $\overline{\ldots}$ denotes an average over the lattice. The equilibrium configuration for the field consists of two phases with values for the field $\psi\approx+1,-1$, deep inside every one of the phases, respectively. These phases will be separated by two planar interfaces (due to the periodic boundary conditions) in the direction of, say, the y axis. The profile of the interface along the y axis will be given (this is only approximately true in a finite system) by the well-known soliton solution

$$\psi(y)=\tanh\left[\frac{y}{\sqrt{2}}\right] .$$

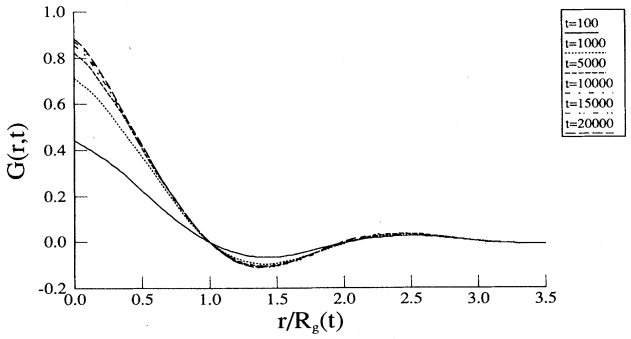

FIG. 4. Spherically averaged pair correlation function as a function of $r/R_g(t)$ to check scaling ansatz Eq. (14). $R_g(t)$ is defined such that this plot goes through the point (1,0). Here, and in subsequent figures, the width Δr, used in the spherical average [see Eq. (16)] is taken equal to $\delta r=1.7$. Scaling holds reasonably well after $t=5000$ although the position of the first minimum decreases systematically at least up to $t=15\,000$ (see Fig. 5).

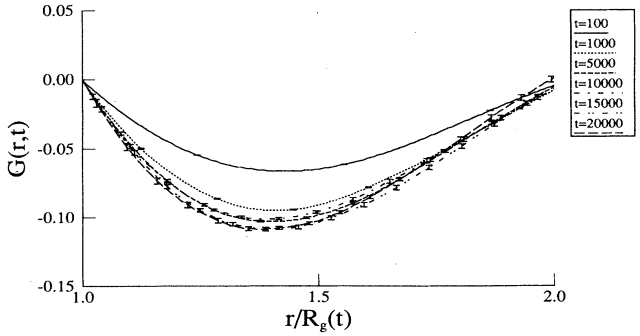

FIG. 5. Details of Fig. 4 near the first minimum of the scaling function.

In a cubic box of linear dimension $L\delta r$ one then has

$$g(0)=\frac{2}{L\delta r}\int_{-\frac{L\delta r}{4}}^{\frac{L\delta r}{4}}\psi^2(y)dy=1-\frac{4\sqrt{2}}{L\delta r}\ , \tag{19}$$

to first order in $1/L\delta r$. In our case $L\delta r=112$ and then $g(0)=0.95$. The value for $g(0)$ at the latest time obtained in our numerical solution is $g(0)=0.88$, which is close but not equal to the asymptotic value. That indicates that for very small values of the scaling variable ρ, the curve in Fig. 4 is not quite yet the true scaling function. Scaling cannot be checked for arbitrary large values of the scaling variable ρ due to the finiteness of the system. The periodic boundary conditions impose a maximum distance on the lattice equal to $L\delta r/2=56$. When $t=20000$, $R_g(t)=26.4$ and the maximum value of the scaling variable ρ for which we can study scaling at this late time is then $\rho=26.4/56=2.12$. We are, however, including in Fig. 4 data up to $\rho=3.5$ in order to show that scaling is very well satisfied for large values of ρ at relatively earlier times.

One can also define a normalized pair-correlation function

$$G_n(r,t)\equiv\frac{G(r,t)}{G(0,t)}\ ,$$

which starts at unity for $r=0$. This would be also a more convenient function to compare with Monte Carlo simulations of the Ising model data in which $G(0,t)\equiv 1$. The scaling function $g_n(\rho)$ derived from $G_n(r,t)$ plotted in Fig. 6.

We also concentrated on the correlation function $G_a(x,t)$ defined in Eq. (17), mainly because there is no uncertainty in the coordinate x for this function in contrast to the case of $G(r,t)$. We show the scaling of $G_a(x,t)$ by plotting this function against $\rho=x/R_a(t)$ in Fig. 7. It is not surprising that there are large error bars associated with $G_a(x,t)$ for large values of x since when x is larger than $R_a(t)$ (which corresponds roughly to the linear size of the domains) the value of the correlation function is small and fluctuates wildly. Unless there are a large number of pairs contributing to the correlation function, the statistical errors become important and are actually comparable to the value of the function itself. We note that for large values of x, the number of pairs contributing to $G_a(x,t)$ is much smaller than the corresponding number contributing to $G(r,t)$, and, hence, $G_a(x,t)$ shows much larger errors than $G(r,t)$ for these large values of x. However, when $x\lesssim R_a(t)$, the correlations are computed for pairs mainly inside bulk domains and the fluctuations in the values of the correlation function are small. Thus, the length $R_a(t)$ calculated from the first zero of $G_a(x,t)$ contains small errors, since $G_a(x,t)$ itself contains small error bars in this range of x values, as evident in Fig. 7. From this figure we conclude that very good scaling holds at least for $t\geq 10000$ and values of $x\lesssim R_a(t)$, whereas large error bars prevent us from commenting about scaling for larger values of $x/R_a(t)$.

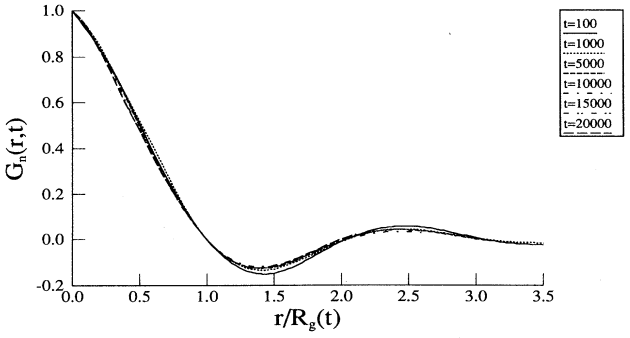

FIG. 6. Same as Fig. 4 for the "normalized" pair-correlation function $G_n(r,t)\equiv G(r,t)/G(0,t)$. Note that now the first minimum is slightly increasing with time.

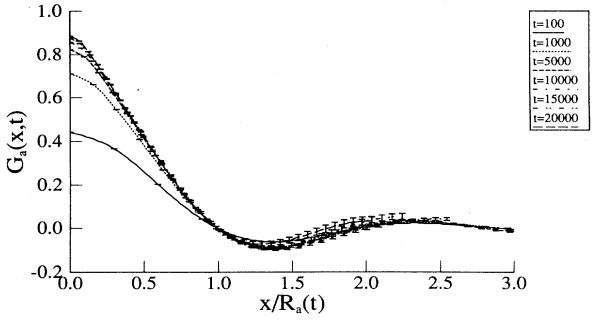

FIG. 7. Plot of the pair-correlation function averaged along the lattice axes vs $x/R_a(t)$ to check scaling ansatz Eq. (14) and possible anisotropy in the scaling functions. $R_a(t)$ is defined such that this plot goes through the point (1,0). The dispersion of values for large values of the abscissa is discussed in the text.

2. *Structure function*

As in the case of the correlation function, we define a spherically averaged structure factor

$$S(k,t)=\sum_{k-(\Delta k/2)<|\mathbf{k}|\leq k+(\Delta k/2)}S(\mathbf{k},t)/n(k,\Delta k)\ , \tag{20}$$

where,

$$n(k,\Delta K)=\sum_{k-(\Delta k/2)<|\mathbf{k}|\leq k+(\Delta k/2)}1\ . \tag{21}$$

The quantity defined in Eq. (21) denotes the number of lattice points in a spherical shell of width Δk, centered around k. In Fig. 8 we show the "raw" data for $S(k,t)$ [with $\Delta k=1(2\pi/L\delta r)=0.056$] for early and intermediate times during the evolution. The development of a Bragg peak related to the coarsening of the domains is qualitatively similar to that observed in previous Monte Carlo simulations of the Ising model[9] and experimental studies of several alloy systems.[1] Figure 9 shows the corresponding data for intermediate to late times. One should note that it is practically impossible to show the two sets of figures in the same scale since the peak height in Fig. 9 is about an order of magnitude larger than that shown in Fig. 8. Also, it is very difficult to locate precisely the position of the peak for very late times due to the

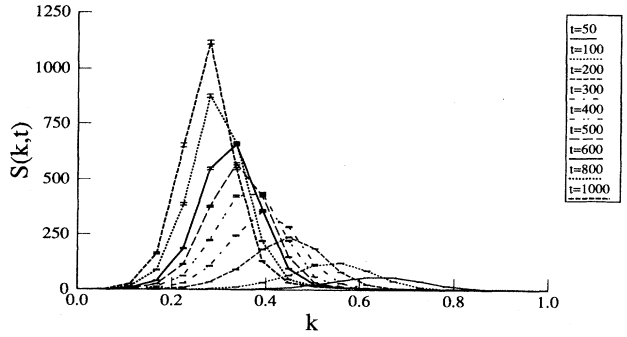

FIG. 8. Spherical average of the structure function, Eq. (12), as defined in Eq. (20) with a value for the width for the spherical average $\Delta k = 2\pi/L\delta r = 0.056$, for early to intermediate times.

finiteness of the lattice used in the study. One could increase the number of points around the peak by decreasing the shell width Δk used in the spherical average, but the statistical errors in the values of $S(k,t)$ are then much larger. We discuss this fact in more detail when analyzing the scaling for the structure function.

The scaling ansatz, Eq. (14) can be tested by plotting $S(k,t)/R(t)^3$ vs $\chi = kR(t)$ and checking whether the resulting functions are independent of time. In Figs. 10 and 11 we show such a plot for late times, using $R_g(t)$ as the scaling length. It is clear from the latter figure that dynamical scaling is well satisfied for relatively large values of the scaling variable χ, say $\chi \geq 4.0$. On the other hand, for small values of χ the lattice discretization does not leave us with enough points to make a conclusive statement about scaling. However, we believe that the asymptotic scaling function will not be significantly different from that shown in Fig. 10. In order to clarify this point we have used a smaller value of

$$\Delta k = 0.25 \left\lfloor \frac{2\pi}{L\delta r} \right\rfloor = 0.01 ,$$

and plotted the resulting scaling function in Fig. 12.

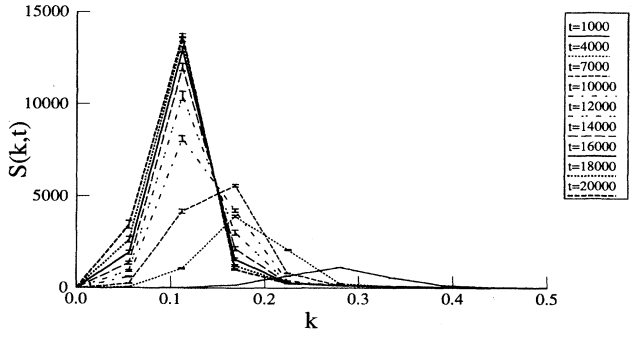

FIG. 9. Same as Fig. 8 for intermediate to late times. Due to the fact that the lattice imposes a discretization in the first Brillouin zone where the wave vectors **k** are defined, it is very difficult to locate precisely the maximum of this function for these times.

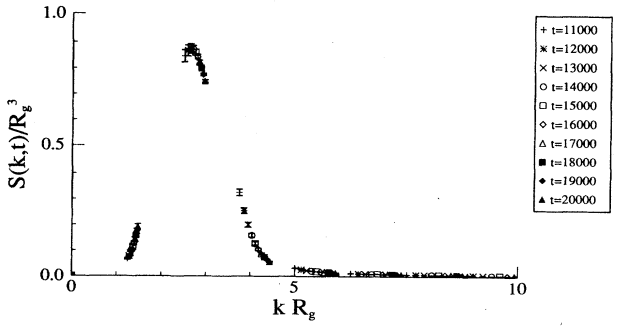

FIG. 10. Spherically averaged structure function $S(k,t)$ plotted to check scaling ansatz Eq. (15) using as scaling length the first zero of the spherically averaged pair-correlation function. An accurate form of the scaling function for small values of the scaling variable cannot be determined precisely due to the finiteness of the lattice used in the numerical study.

When $\chi \geq 3.5$, the scaling function is independent of the shell width. For small values of χ, however, there is a systematic difference between the two functions. It seems plausible that the scaling function with smaller value of Δk represents a better approximation to the "true" scaling function, although the data contain larger error bars and, thus, do not allow us to make a more definitive statement.

We note that it is difficult to perform a quench at exactly the critical concentration in real materials, due in part to the fact that for many mixtures the coexistence curve is not well known or is asymmetric. Numerical studies have provided, until now, the only unquestionable critical quenches. We have compared the scaling function with previous Monte Carlo data as well as some other theoretical and phenomenological results. There appears to be systematic differences as follows: the scaling functions computed in this study are narrower around the maximum than that observed in the Monte Carlo study.[9] Although it is difficult to compare time scales of the two different models, due to the inherent coarse-grained nature of the CHC model, we believe that the latest time of evolution studied in the Monte Carlo simula-

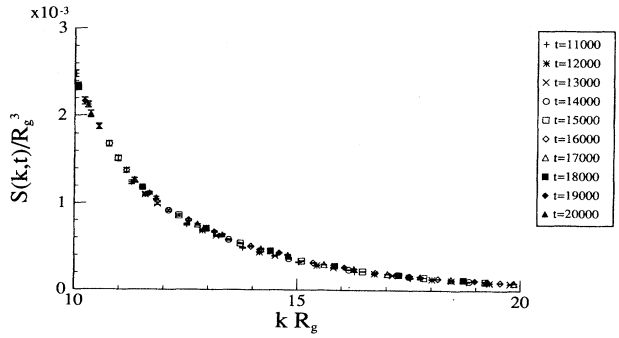

FIG. 11. Details of Fig. 10: For the large values of the scaling variable plotted here we can determine very precisely the predicted form of the scaling function.

tions for the "deep" critical quenches (less than 2000 Monte Carlo steps) is simply too small to be in the scaling regime (this is also supported by the fact that in two dimensions[10] one needs to run for at least 40 000 Monte Carlo steps to enter the scaling regime). We have suitably rescaled the axes in Fig. 12 such that the peak is located at coordinates (1,1) in order to compare with the phenomenological expression for the scaling function introduced by Furukawa.[25] We find that this form does not agree with our data. Also, the scaling function predicted in a recent field-theoretical low temperature expansion[13] is not consistent with our scaling function.

3. *Growth law*

Apart from the previously defined lengths, $R_g(t)$ and $R_a(t)$, a measure of the typical domain size can be defined as the inverse of the moment $k_a(t)$ of the spherically averaged structure function

$$k_a(t)=\sum_k kS(k,t)\Big/\sum_k S(k,t)\ . \tag{22}$$

The characteristic length scale $R(t)$ given by any of the preceding measures, is expected to behave as t^a for sufficiently late time t. The classical theory of Lifshitz and Slyozov,[6] valid only in the limit where the volume fraction occupied by droplets goes to zero, i.e., near the coexistence curve in the nucleation regime, predicts $a=\frac{1}{3}$ independent of the dimension. The Lifshitz-Slyozov theory, based on a mechanism of evolution governed by bulk diffusion across the interfaces, has been qualitatively extended[26] to the case of equal volume fraction of the two phases with the prediction $a=\frac{1}{3}$. On the other hand, a recent theoretical study of the dynamics[12,13] (combined with numerical simulations) predicts $a=\frac{1}{4}$ for a critical quench in two and three dimensions. For two-dimensional systems, recent numerical studies of the

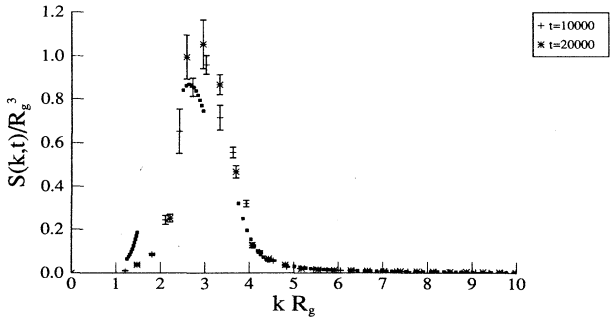

FIG. 12. Scaling function as derived from the spherically averaged structure function using a bin size $\Delta k=0.25(2\pi/L\delta r)=0.014$ [see Eq. (20)] for $t=10\,000$ and $t=20\,000$. The solid symbols represent the points plotted in Fig. 10. We see that for small values of the scaling variable $kR_g(t)$, there are some systematic differences. When $kR_g(t)>3.5$, however, both curves coincide.

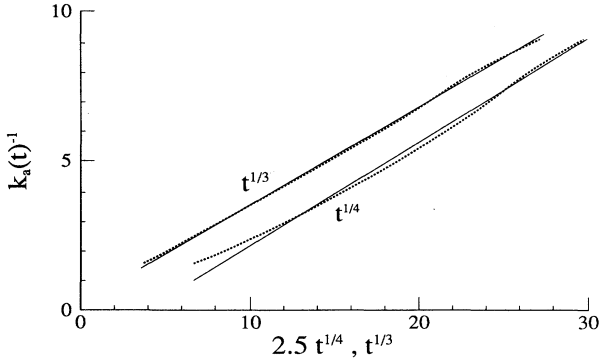

FIG. 13. Domain size as given by the inverse of the first moment of the spherically averaged structure function [see Eq. (22)] as a function of $t^{1/3}$ and $2.5t^{1/4}$.

Cahn-Hilliard equation with and without thermal noise,[15,16] the kinetic Ising model with Kawasaki dynamics[10] and a cell dynamics approach,[17,18] all yield $a=\frac{1}{3}$ and show that these models actually belong to the same dynamical universality class.[19] In three dimensions the situation is not clear. Experiments in various systems have been analyzed in terms of effective exponents a which lie in the range 0,15–0.37.[1,27] In the Monte Carlo studies of the kinetic Ising model in three dimensions,[9] the authors interpreted their results for the domain size in terms of an effective exponent in the range 0.19–0.35, the smaller exponents corresponding to the critical quenches, although the authors claimed that the data are always compatible with $a=\frac{1}{3}$.

Figures 13–15 show different measures of the characteristic length plotted against $t^{1/3}$ and $t^{1/4}$. Although it is, of course, difficult to distinguish between exponents $\frac{1}{3}$ and $\frac{1}{4}$ since their difference is small, the presented figures show that $R(t)=c+dt^{1/3}$ is a slightly better global fit than $R(t)=c+dt^{1/4}$. This visual demonstration is not, certainly, the best way of extracting a growth law ex-

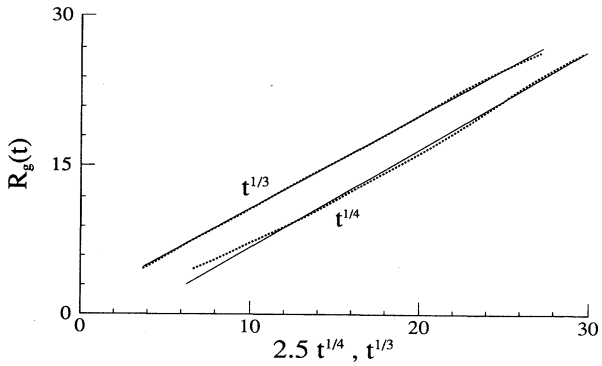

FIG. 14. Same as Fig. 13 for the domain size $R_g(t)$ defined as the first zero of the spherically averaged pair-correlation function.

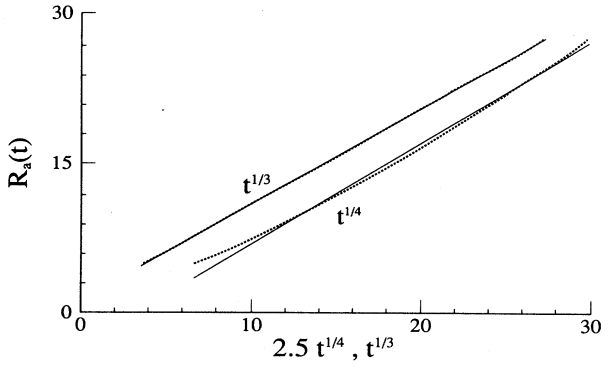

FIG. 15. Same as Fig. 13 for the domain size $R_a(t)$ defined as the first zero of the pair-correlation function averaged along the lattice axes.

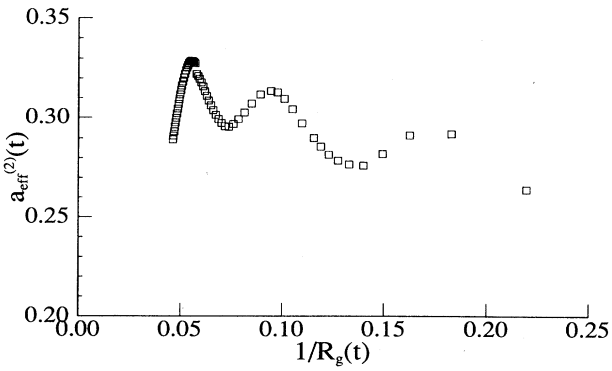

FIG. 17. Effective exponent $a_{\rm eff}^{(2)}(t)$ as defined in Eq. (24) for the measure $R_g(t)$ of the domain size. Note the wild fluctuations in the value of the effective exponent.

ponent. If the predictions of the different theories were a mere $R(t)=dt^a$, then a log-log plot of $R(t)$ vs t would have been sufficient to determine a. In any theory, though, the prediction $R(t)\approx t^a$ is only an asymptotic result, allegedly valid only for very late times. The main problem is that, usually, the corrections to this asymptotic law are not well known, nor are their relative (numerical) importances well established. An argument due to Huse[26] identifies the predominant correction to the main mechanism in the Lifshitz-Slyozov theory as the effect of transport along the interfaces (a similar idea was proposed earlier by Furukawa[28]) and provides a semiquantitative expression for the correction term (in the asymptotic limit) as an additive constant to the simple power law, i.e, $R(t)=c+dt^{1/3}$. Although the original calculation of Huse was done for the Ising model, the argument is probably applicable to the Cahn-Hilliard model we are discussing here. We have tried to find the best fit of our data to the more general expression $R(t)=c+dt^a$. This three-parameter fit is an extremely difficult task. The values of the fitted parameters depend on the time interval chosen for the fitting procedure. This is particularly true for the measure $R_g(t)$. Also, if the time interval is not large enough, one can encounter unphysical values for the parameters. We have found the best fit for $50\le t\le 20\,000$ for $R_g(t)$ to be $c=0.54$, $d=1.14$, and $a=0.32\pm0.02$. For $R_a(t)$ and $k_a(t)^{-1}$, the best fits over the same time interval are $c=1.36$, $d=0.94$, $a=0.337\pm0.008$, and $c=0.44$, $d=0.27$, and $a=0.35\pm0.03$, respectively. The errors are based purely on the statistical errors of the different lengths, without taking into account the possible inherent systematic errors in $R_g(t)$ and $k_a(t)^{-1}$.

Another equivalent yet illuminating way of extracting a growth law exponent is to define an effective exponent[26,29]:

$$a_{\rm eff}(t)=\frac{d\ln R(t)}{d\ln t}=a-\frac{ca}{R(t)}\ , \tag{23}$$

such that a plot of $a_{\rm eff}$ versus $1/R(t)$ should give a straight line whose intersection at the origin is the exponent a. This logarithmic derivative is done in practice by using

$$a_{\rm eff}^{(\alpha)}(t)=\frac{\log_\alpha R(\alpha t)}{\log_\alpha R(t)}\ . \tag{24}$$

Typical values for α used by previous authors are $\alpha=2$ Ref. 10 and $\alpha=10$.[26] Figures 16 and 17 show the

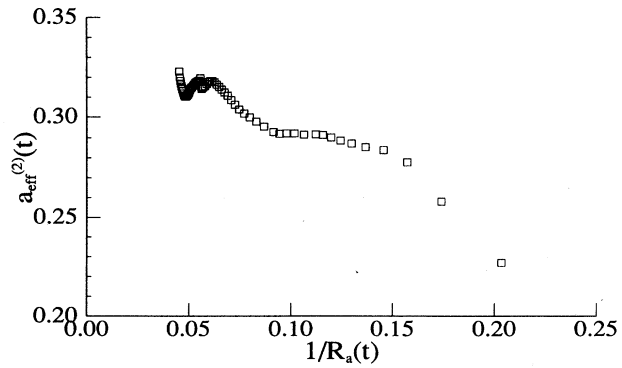

FIG. 16. Effective exponent $a_{\rm eff}^{(2)}(t)$ as defined in Eq. (24) for the measure $R_a(t)$ of the domain size.

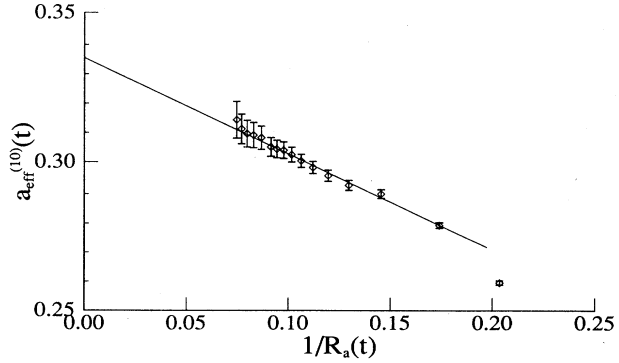

FIG. 18. Effective exponent $a_{\rm eff}^{(10)}(t)$ as defined in Eq. (24) for the measure $R_a(t)$ of the domain size. The ordinate of the straight-line fit at the origin is $a=0.335$.

effective exponent when $\alpha=2$, for measures $R_g(t)$ and $R_a(t)$, respectively. The wild fluctuations in the value of the effective exponent calculated from $R_g(t)$ [as compared with that from $R_a(t)$] indicate that $R_g(t)$ is less well behaved than $R_a(t)$. Although the data are very noisy it seems that the effective exponent is always above $\frac{1}{4}$ with the general tendency that $a_{\text{eff}}(t)$ increases with time. We also present the effective exponent for $R_a(t)$ using $\alpha=10$ in Fig. 18. The extrapolation to the origin gives $a=0.335\pm0.010$.

IV. CONCLUSIONS

In this paper we have studied numerically a complicated stochastic nonlinear partial differential equation appropriate for modeling the dynamics of phase separation and pattern formation in a variety of systems undergoing the process of spinodal decomposition. An accurate solution of this equation requires the introduction of a space discretization with a very large number of lattice points and a relatively small time step. Also, in order to confirm theoretical ansatzs concerning the scaling behavior of the system, it is necessary to solve the equation up to a very late time. Finally, the stochastic nature of the equation (implemented here by the use of different random initial configurations for the concentration field) requires an average over many realizations. This problem thus belongs to the category of those needing an extensive use of the resources (both memory and CPU) of powerful supercomputers. The present study used about 300 h of Cray model X-MP-48 central-processing-unit time.

In this study we have focused on late-time behavior for a reasonably large system. We find that, at sufficiently late times, the scattering intensity and the pair-correlation functions are well represented in terms of scaling with a time-dependent length. Our analysis of the time dependence of this characteristic length supports a modified Lifshitz-Slyozov law in which the asymptotic growth law exponent is $\frac{1}{3}$. However, a definitive numerical calculation of this controversial exponent would require data spanning much larger times. Also, the exact form for the scaled structure function around the maximum can only be attained in studies involving much larger systems.

ACKNOWLEDGMENTS

We thank Joel Welling of the Pittsburgh Supercomputing Center for much help with the graphics used in Fig. 1. This work was supported by National Science Foundation (NSF) Grant No. DMR-8612609 and by an NSF grant of computer time at the Pittsburgh Supercomputing Center. One of us (R.T.) acknowledges partial financial support from US/Spain Grant No. CCB-8402/025.

*Present address: Department of Physics, Lehigh University, Bethlehem, PA 18015.

†Present address: Departament de Física, Universitat de les Illes Balears, Palma de Mallorca, E-07010, Spain.

[1]For a review, see J. D. Gunton, M. San Miguel, and P. S. Sahni, in *Phase Transitions and Critical Phenomena,* edited by C. Domb and J. L. Lebowitz (Academic, London, 1983), Vol. 8.

[2]J. W. Cahn and J. E. Hilliard, J. Chem. Phys. **28**, 258 (1958); H. E. Cook, Acta Metall. **18**, 297 (1970).

[3]J. S. Langer, Ann. Phys. **65**, 53 (1971).

[4]J. S. Langer, M. Bar-on, and H. D. Miller, Phys. Rev. A **11**, 1417 (1975).

[5]M. Grant, M. San Miguel, J. Viñals, and J. D. Gunton, Phys. Rev. B **31**, 3027 (1985).

[6]I. M. Lifshitz and V. V. Slyozov, J. Phys. Chem. Solids **19**, 35 (1961).

[7]J. A. Marqusee and J. Ross, J. Chem. Phys. **79**, 373 (1983); **80**, 536 (1984); J. A. Marqusee, *ibid.* **81**, 976 (1984); M. Tokuyama, Y. Enomoto, and K. Kawasaki, Physica **143A**, 183 (1986), and references therein.

[8]For a recent review, see P. W. Voorhees, J. Stat. Phys. **38**, 231 (1985).

[9]J. L. Lebowitz, J. Marro, and M. H. Kalos, Acta Metall. **30**, 290 (1982), and references therein.

[10]J. G. Amar, F. E. Sullivan, and R. D. Mountain, Phys. Rev. B **37**, 196 (1988).

[11]Z. W. Lai, G. F. Mazenko, and O. T. Valls, Phys. Rev. B **37**, 9481 (1988).

[12]G. F. Mazenko and O. T. Valls, Phys. Rev. Lett. **59**, 680 (1987).

[13]G. F. Mazenko, O. T. Valls, and M. Zannetti, Phys. Rev. B **38**, 520 (1988).

[14]C. Roland and M. Grant, Phys. Rev. Lett. **60**, 2657 (1988); K. Kaski and J. D. Gunton (unpublished); J. D. Gunton, E. T. Gawlinski, and K. Kaski, in *Dynamics of Ordering Processes in Condensed Matter,* edited by S. Komura (Plenum, New York, 1988).

[15]E. T. Gawlinski, J. D. Gunton, and J. Viñals (unpublished).

[16]T. M. Rogers, K. R. Elder, and R. C. Desai, Phys. Rev. B **37**, 9638 (1988).

[17]Y. Oono and S. Puri, Phys. Rev. Lett. **58**, 863 (1987).

[18]A. Chakrabarti and J. D. Gunton, Phys. Rev. B **37**, 3798 (1988).

[19]J. D. Gunton, E. T. Gawlinski, A. Chakrabarti, and K. Kaski, C, J. Appl Cryst. (to be published).

[20]R. Toral, A. Chakrabarti, and J. D. Gunton, Phys. Rev. Lett. **60**, 2311 (1988).

[21]P. C. Hohenberg and B. I. Halperin, Rev. Mod. Phys. **43**, 435 (1977).

[22]K. Oki, H. Sagana, and T. Eguchi, J. Phys. (Paris) Colloq. **7**, C-414 (1977).

[23]K. Binder, Z. Phys. B **43**, 119 (1981).

[24]K. Binder and D. Stauffer, Phys. Rev. Lett. **33**, 1006 (1974).

[25]H. Furukawa, Physica **123A**, 497 (1984), and references therein.

[26]D. A. Huse, Phys. Rev. B **34**, 7845 (1986).

[27]B. D. Gaulin, S. Spooner, and Y. Morii, Phys. Rev. Lett. **59**, 668 (1987), and references therein.

[28]H. Furukawa, Adv. Phys. **34**, 703 (1985).

[29]M. E. Glicksman and P. W. Voorhees, Metall. Trans. A **15**, 995 (1984).